Modelling and optimisation of ENi-P-TiO2 coatings synthesised with Zwitterionic surfactant on naval grade AH36 Steel

Article *in* Sadhana · June 2022

DOI: 10.1007/s12046-022-01890-7

CITATIONS
4

READS
33

5 authors, including:

R. Anthoni Sagaya Selvan
Defence Institute of Advanced Technology
7 PUBLICATIONS **16** CITATIONS
SEE PROFILE

D. G. Thakur
Defence Institute of Advanced Technology
103 PUBLICATIONS **1,377** CITATIONS
SEE PROFILE

M. Seeman
Annamalai University
42 PUBLICATIONS **292** CITATIONS
SEE PROFILE

Muraliraja Rajaraman
Vels University
36 PUBLICATIONS **937** CITATIONS
SEE PROFILE

Sādhanā (2022)47:116
https://doi.org/10.1007/s12046-022-01890-7

Modelling and optimisation of ENi-P-TiO_2 coatings synthesised with Zwitterionic surfactant on naval grade AH36 Steel

R ANTHONI SAGAYA SELVAN[1,*], DINESH G THAKUR[1], M SEEMAN[2], R MURALIRAJA[3] and MOHD. IMRAN ANSARI[4]

[1]Department of Mechanical Engineering, DIAT (DU), Pune, India
[2]Centre for Materials Joining and Research (CEMAJOR), Department of Manufacturing Engineering, Annamalai University, Annamalai Nagar 608002, India
[3]Department of Mechanical Engineering, VISTAS, Chennai, India
[4]Department of Robotics and Automation, Bharati Vidyapeeth (DU) College of Engineering, Pune 411043, India
e-mail: selvanras@gmail.com; dinnu74@yahoo.com; mfgseeman@gmil.com; muralimechraja@gmail.com ; imransarimech@gmail.com

MS received 18 October 2021; revised 6 March 2022; accepted 18 April 2022

Abstract. There are two primary objectives of this study to design the titanium-based novel ENi-P composite coatings on naval grade AH36 steel through Taguchi DOE with the addition of Zwitterionic surfactant and identify the most significant factor which contributes to the enhancement of microhardness in the fabricated coatings. The L9 composite coatings are developed by varying bath temperature, pH, wt% of C14-SB and TiO_2 nanoparticles in the electroless bath. Each coatings elemental composition is investigated using SEM and EDAX analysis. XRD peaks are matched with the peaks of Nickel, Phosphorous and Titanium contents in the deposits. The ANOVA and the S/N ratio were deduced and utilised to formulate the optimal combination of parameters for enhancing microhardness in the coatings. The predicted optimal coatings were validated with a confirmation run and achieved 54.66% microhardness enhancement compared with the initial condition and 196.4% improvement achieved with the substrate material AH36 steel. This experimental work proves its first kind of titanium-based ENi-P coating over the marine grade AH36 steel substrate closely associated with defence applications.

Keywords. AH36 steel; ENi-P-TiO_2 composite coatings; zwitterionic C14-SB surfactant; bath pH group; microhardness.

1. Introduction

The AH36 steel is high strength steel used in shipbuilding, and these steel plates are normalised, control rolled, and thermomechanically processed before the shipbuilding. The addition of aluminium, vanadium, and niobium in the steel resulted in a fine-grained microstructure [1]. It is generally used for naval and cargo shipbuilding, which is continuously exposed to cyclic stresses due to frequent loading and unloading of cargos, engine vibration, shock, and vibration due to firing heavy guns and artilleries. In addition, the continuous ship's motion through rough waves and high windy environment causes the ships to reach as high as 10^8 cycles within 20 years of sea life [2]. The marine-grade AH36 steel plates are generally used in shipbuilding to fabricate hull and structural members, including shell plating. Such steel is also usually used in fabricating sea tubes for seawater inlets for various machinery and high capacity pumps, including the fabrication of high-velocity waterjet inlet duct tunnels. However, the most frequently stated problem observed on the marine components is the combinative impact of high-velocity seawater and sand particles on these steel surfaces, usually thinning down the surface due to erosive wear [3]. This issue has received considerable attention in the marine and naval fraternities to avoid and minimise such erosive degradation from the material surface. Hence, specific underwater antifouling and anti-corrosive paints are currently being applied on such surfaces for restoration during the ship's regular time based on planned underwater maintenance schedules. However, a major problem with this kind of approach is that the actual resistance of underwater paints is usually not sustainable against cavitation and erosive wear due to the regular impact of high-velocity incoming seawater with

*For correspondence
Published online: 15 June 2022

foreign particles [4]. Though many surface modifications are currently under practice to improve the ship's operational and fighting capability, nil studies have investigated the application of the novel electroless coating on the marine grade AH36 steel in the past. Hence, this prospective study was designed to investigate the use of electroless coating for marine applications in the future. The electroless coating was an innovative technique gifted to humankind by Brenner and Riddle [5]. The name itself imparts that this coating does not require any external power supply. It is considered a functional coating due to its combined resistance against both corrosion and wear. The ability of its uniform thickness over the entire part/component, irrespective of its size and shape, made many industries opt for this novel technique for various applications [6].

Hardness is considered one of the distinctive properties that played a significant role in civilisation evolution by manufacturing various equipment and structures. The maiden material hardness is introduced by Brinell [7]. The measuring ability of any solid material to resist change of its shape against applied compressive force is termed as the hardness of the material. Variety of deformation can be achieved through indentation, cutting process, bending, scratching, and wear. Moreover, hardness is related to mechanical properties like ductility, fatigue resistance, and strength; hence, hardness testing is considered as a straightforward way of controlling material quality in the industry. The hardness measurement is considered as an inexpensive and rapid method to evaluate comprehensive mechanical property due to its simple correlation between hardness and strength characteristics. On the other hand, the hardness test is also famous because it is economical compared to skilful tensile experiments [8]. Surface hardness is indispensable for any components and half-finished products to perform wear and tear actions. Hence, custom-made hard materials/surfaces to satisfy the specific functional requirement stimulated the invention of numerous surface modification techniques. ENi-P deposition gained its superiority over others due to its unique nature [9]. Further, the hardness of the ENi-P coating can also be achieved by incorporating hard and soft particles like SiC, B_4C, Al_2O_3, ZnO_2 and TiO_2 as per the specific industrial requirement [10]. The third element of hard or soft particles in the ENi-P matrix is termed composite coatings. Electroless composite coatings are fabricated by allowing the adsorption of particles on the substrate surface and consequent deposition of matrix material on the surface [11]. It is now effectively established from previous research that embodying nano-particles in the autocatalytic Ni-P deposits improved their surface properties and performance in various applications [12]. Alirezaei *et al* [13] have studied and reported that adding alumina particles in the Ni-P matrix increases the hardness of the composite coatings due to the barrier functioning of alumina particles embedded in the Ni-P deposition. Araghi *et al* [14] reported that incorporating B_4C particles in the Ni-P-B_4C composite coatings enhanced the hardness of the coatings due to the restriction offered by B_4C particles for dislocation movement of the coatings. Novakovic *et al* [15] reported that the hardness of Titanium-based ENi-P composite deposition depends on the bonding between titania particles and the Ni-P matrix. Allahkaraml *et al* [16] reported that the higher hardness in the ENi-P-TiO_2 composite coating increases with the complementary addition of TiO_2 particles in the Ni-P matrix. Hamid *et al* [17] reported that the hardness enhancement in the ENi-P-WC composite deposition is achieved by incorporating WC particles in the coating. Chen *et al* [18] fabricated Ni-P-TiO_2 composite coating through the sol-gel technique and achieved higher microhardness and wear resistance than the titanium-based composite deposition. Tamilarasan *et al* [19], through Taguchi optimisation, achieved reduced corrosion rate and higher microhardness through the optimal coating by 70% than the base metal, and further he reiterated that the surfactant type and its concentration contributes to the ENi-P-TiO_2 coating properties. Interestingly, Imtiaz Ahmed Shoib *et al* [20] fabricated electroless Ni-P-TiO_2 coatings on aluminium alloy through machine learning approaches to achieve optimal microhardness in the coatings. Surfactants are mixed into the electroless nickel bath to lower the surface tension to better spread and reduce the interface tension between the liquids or between solid particles and liquid phases [21]. Elansezhian *et al* [22] stated that additions of (SDS and CTAB) surfactant in the ENi-P bath enhanced the coating hardness by up to 50% due to the formation of mixed amorphous and crystalline structure in the coated surface. Muraliraja *et al* [23] studied the influences of Zwitterionic surfactant. They reported that the microhardness of the coating enhances with the weight addition of the surfactant up to CMC level, and further addition above CMC reduces the microhardness due to the higher nickel content in the deposition. While considering the previous studies, the research on ENi-P depositions for enhancing microhardness has been mostly restricted to limited comparisons of various anionic and cationic surfactants, the addition of third element, optimal bath loading, bath temperature, reducing agent, and stabilisers. This indicates a need to explore the newer input factors combinations during the design and fabrication of ENi-P composite coatings for various applications.

This investigation aims to design and optimise the microhardness of the AH36 steel surface through the deposition of ENi-P-nano TiO_2 composite coatings with the addition of a zwitterionic surfactant. Hence, Taguchi L9 orthogonal arrays have been formulated to identify the specific contributions of bath temperature and pH, the weight of zwitterionic surfactant and TiO_2 nano-particles to achieve maximum hardness in the coated surface. Through ANOVA, the input process factors were analysed for their detrimental contribution and their interaction effects to achieve the maximum hardness in the coatings. Also, the

derived S/N results correlate with the ANOVA output to confirm the experimental results. Further, the XRD profiles are studied to evaluate various phases in initial and optimal coatings. Additionally, the EDAX analysis evaluated the percentage of individual elements deposited on the coatings and their contributions to achieving respective microhardness in the coated surface.

2. Experimental procedure and details

2.1 *Coating preparations*

The substrate in this study is fabricated from high strength marine-grade steel AH 36. The chemical composition and its mechanical properties are tabulated in table 1. All the specimens were fabricated from a single steel plate duly certified by the Indian register of shipping for the shipbuilding. The substrate dimensions are (25 × 25 × 5.85) mm. Once the samples were fabricated from the source plate, they were first grounded and then polished with 600, 800, 1000, 1200, and 2000 grit SiC papers. Before commencing the deposition process, the polished substrates are initially subjected to a pre-treatment process of 10 minutes of ultrasonic cleaning with acetone, 2 min dipping in ethanol, and finally, 1-minute acid pickling with a 10% sulphuric acid bath. Following the pre-treatment process, the samples are thoroughly cleaned with demineralized water before and after all pre-treatment processes and before dipping the substrate in the deposition process. The chemical composition of the ENi-P bath is tabulated in table 2.

The reducing agent reduces the metal ions donated by the nickel source. Trisodium citrate dehydrates blended as a complexing agent to form metastable nickel complexes, attributing to the slow down and steady-state reaction. Ammonium chloride was added as a buffering agent to maintain the bath pH and prevent the sudden drop during the deposition process. Additionally, liquid ammonia maintains the required pH level (4,6,8) in the electroless bath. Zwitterionic detergent [3-(N, N- Dimethylmyristylammonio) propanesulfonate] from Sigma-Aldrich with ≥ 99% (TLC) was used as the surfactant. Before introducing into the bath, nano TiO_2 powder and surfactants were ultrasonically agitated separately for 15 min, and the concentrate was then carefully infused into the main bath. After the coating process, the substrates are dried, and coating thickness is measured for all the substrates.

Table 2. Bath composition and parameters.

Chemicals	Brand	Quantity
$N_aH_2PO_2{\cdot}H_2O$	Merck	35 g/L
$NiCl_2{\cdot}6H_2O$		30 g/L
$C_6H_5Na_5O_72{\cdot}H_2O$		50 g/L
NH_4Cl		50 g/L
Duration of deposition		60 min
Bath volume		400 ml
Stirring speed		500 RPM

2.2 *Hardness measurement*

This study investigated the coating hardness to examine the impact of input parameters. Therefore, the average of 5 readings is taken as the final value. In addition, the microhardness value of AH36 steel substrate hardness was measured and compared with the previous work. The microhardness of the base metal is 197 HV_{200}. The microhardness of acidic and alkaline ENi-P coatings is also measured and compared with the optimal coating, and the contribution of phosphorous, nickel, and titanium in the coatings is verified through EDAX and XRD analyses. The Vicker microhardness of L9 electroless ENi-P-TiO_2 on AH36 marine grade steel is measured per the ASTM E384-16 through a pyramid-shaped indenter provided a 136° apex angle between the opposite sides and square base. A 200-gram force load was applied at the rate of 50μm/s with 10 seconds dwell time, and observed that indentation depth for all the specimens was found to be 1/10th higher than the coating thickness to avoid mechanical contribution from the substrate [24].

2.3 *Design of experiment*

The benefit of using the Taguchi technique is its effectiveness while formulating high standard, reliable systems built on with the help of orthogonal arrays. This technique's

Table 1. Cast analysis and mechanical properties of AH 36.

Heat no.	C	Mn	S	P	SI	AL	Cu	Ti	V	Nb	N	MAE	CE
21400280	0.177	1.222	0.0044	0.012	0.016	0.042	0.006	0.017	0.004	0.020	0.0053	0.041	0.385

Mechanical properties for batches

YS (MPa)	UTS (MPa)	Young modulus (MPa)	Specification
432	524	2×10^5	IS 2062 E 350 C 2011

significant advantages allow us to perform minimal experiments from the complete factorial design with an orthogonal array, which genuinely allows only minimal required experiments from the complete factorial design for the designed process factors. Thereby bypassing many experimental combinations with an optimal setting of process control parameters [25]. It establishes an interpreted approach with a simple and efficient way to determine the optimum range of system design to provide better quality with reduced computational cost. Four input process factors, each consisting of 3 levels, are chosen to determine the significant factors that affect the hardness of the composite coatings. The corresponding L9 orthogonal distribution is tabulated in table 3. In this approach, Genichi Taguchi [26] adopted the signal-to-noise ratio (S/N) as a loss function to measure the quality attributes deduced from the ratio of control factors to noise factors. The higher the positivity of the S/N ratio, the more is acceptable quality. Hence, three distinct ways are adopted to transform from loss function to S/N ratio for evaluating the system's response. They are higher is better (HB), nominal is best (NB), and smaller is best (SB). However, HB characteristics are adopted for maximising the hardness of the coatings. The S/ N ratio for more significance is defined by

$$\mathrm{S/N} = -\log 10 \frac{\Sigma \frac{1}{y2}}{n} \tag{1}$$

where 'y' is the hardness value, and 'n' is the number of experiments. In addition, a statistical method of (ANOVA) analysis is performed to predict the optimal combinations of the process parameters.

2.4 *Analysis of variance (ANOVA)*

ANOVA effectively identifies influential input factors and their considerable interactions in optimising the desired coating output through F-value and *P* value. F-value is deduced by dividing the variance of the factors by the square of errors. Thus, the higher the value indicates the largest its contribution. On the other hand, the P-value suggests the principle of the null hypothesis, considering 0.05 is an upper limit to decide whether to accept or reject [27].

Table 3. Factors and their respective levels.

Process factors	Unit	Levels		
		1	2	3
Bath temperature (A)	°C	80	84	88
Bath pH (B)		4	6	8
C14SB concentration (D)	g/L	0.009	0.018	0.027
Nano TiO_2 (D)	g/L	0.25	0.5	0.75

2.5 *Morphological surface analyses and composite study*

The optimal coating realised from the DOE is characterised through SEM, EDAX, and PXRD analyses. The SEM analysis is utilised to ascertain the surface morphology of the deposited layers conducted through VEGA 3 INCA software in the TESCAN OXFORD machine. The various phases in the coating are verified through PXRD in the Malvern Panatical machine, probing with Cu Kα radiation of 2θ from 10° to 90° with the Step Size of 0.0390° (2θ). Several reports have shown that the properties and structure of as-deposited ENi-P coatings mainly influenced the phosphorous content in the coated surface. Therefore the deposited specimens are examined by varying the process parameters like bath temperature, bath pH, weight addition of Zwitterionic surfactant, and TiO_2 nanoparticles in the electroless composite bath. In addition, EDAX evaluation is carried out on the specimens to confirm the content of Phosphorous, Nickel, and TiO_2, as earlier reported by Sahil Julka *et al* [28].

3. Results and discussion

3.1 *Analysis of signal to noise ratio*

Taguchi optimisation is based on the S/N ratio as introduced earlier. Figure 1 shows the S/N ratio of each input factor and their levels. The most excellent S/N ratio from each factor between their assigned levels suggests the optimal level of that particular factor. The difference between the higher and lower value of the individual S/N ratio is the Delta value for the corresponding factor. From figure 1, we can see that the S/N ratio for higher the better is maximal for level 1 for bath Temperature, level 3 for bath pH, C14SB concentration, and nano-TiO_2 is observed. From this, it is clear that the A1B3C3D3 is the optimal parameter combination to achieve the highest hardness in the coatings. Further, the same can be established from the 3rd run [80, 8, 0.027, 0.75] of the experiment tabulated in table 4. The corresponding microhardness value for the optimal combination is measured as 584 HV_{200}.

From figure 1, we can establish the factor which largely contributes to and governs the microhardness of the ENi-P-TiO_2 composites deposits through their relative position from the mean value. Accordingly, the individual factor coordinates approaching the mean or horizontal line indicate its minimal/ nil contribution to responsive coating hardness. In contrast, the input factors, i.e., bath temperature, bath pH, C (C14-SB concentration), contribute most, hence considered the most determinant factors for achieving the higher microhardness in the ENi-P-nano TiO_2 coatings. The response table for the S/N ratio also further confirms the same through table 5. Also, figure 2 displays

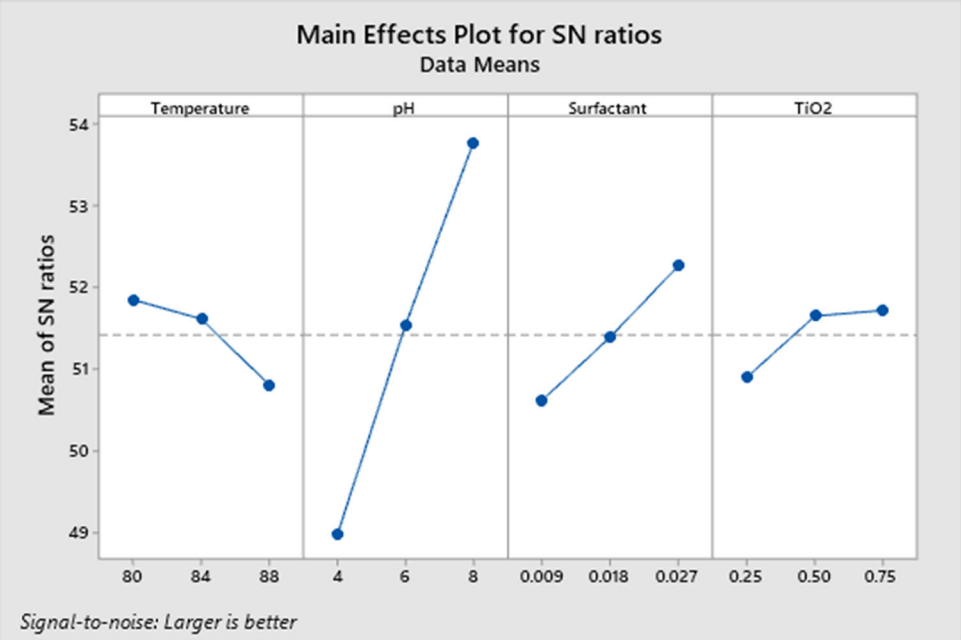

Figure 1. Main effects plot for S/N ratios hardness factor.

Table 4. Response of coatings

Run	Temperature °C (A)	Bath pH (B)	Zwitterionic surfactant g/L (C)	TiO_2 g/L (D)	Microhardness	
					HV_{200}	S/N ratio
T-1	80	4	0.009	0.25	253	48.0624
T-2	80	6	0.018	0.50	405	52.1491
T-3	80	8	0.027	0.75	584	55.3283
T-4	84	4	0.018	0.75	296	49.4258
T-5	84	6	0.027	0.25	400	52.0412
T-6	84	8	0.009	0.50	466	53.3677
T-7	88	4	0.027	0.50	304	49.4558
T-8	88	6	0.009	0.75	331	50.3966
T-9	88	8	0.018	0.25	426	52.5882

Table 5. Response table for the signal to noise ratio hardness.

Level	Temperature (A)	pH (B)	Surfactant (C)	TiO_2 (D)
1	51.85	48.97	50.61	50.90
2	51.61	51.53	51.39	51.65
3	50.80	53.76	52.27	51.72
Delta	1.04	4.79	1.66	0.82
Rank	3	1	2	4

the normal probability plot of the residuals for specimen microhardness value. It can be noticed that the residuals coordinates are located on a straight line, which suggests that the errors are normally distributed, and the regression model is adequate [29, 30].

3.2 *ANOVA*

The individual factor contribution in percentage reveals its weight during their interactions to attain the desired higher hardness in the coatings. Larger the percentage contribution in main effects confirms its decisiveness to obtain the higher microhardness in the coating. From ANOVA analysis, it established that bath pH, i.e., parameter (B), has shown a substantial contribution of 78.95%, followed by the weight addition of Zwitterionic Surfactant

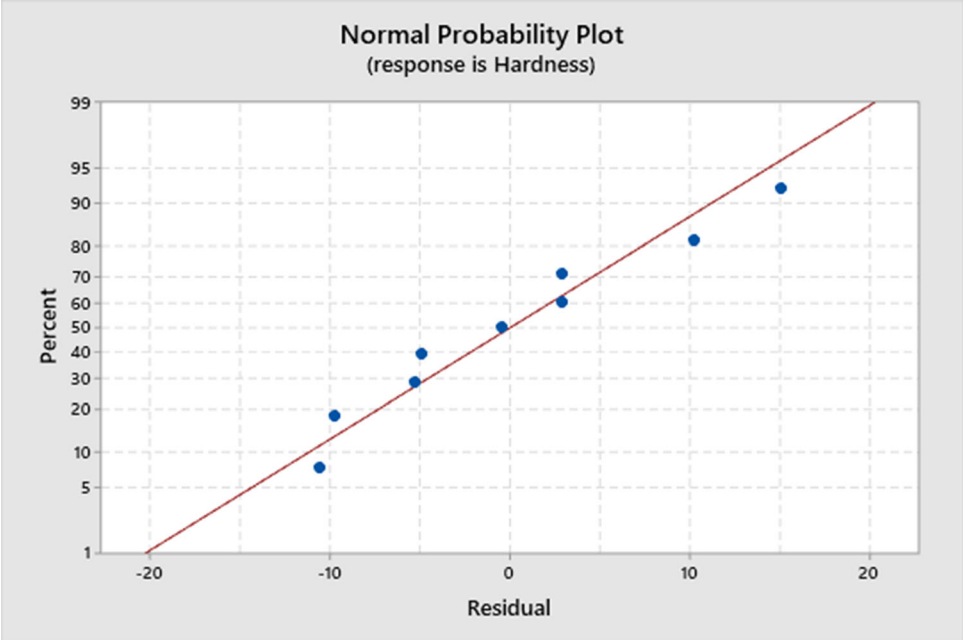

Figure 2. Residual plots as hardness is a responsive parameter.

Table 6. Analysis of variance for microhardness.

Source	DF	Adj SS	Adj MS	F-value	*P* value
Regression	4	84034.3	21008.6	138.09	0.000
Temperature	1	5953.5	5953.5	39.13	0.003
pH	1	66360.2	66360.2	436.18	0.000
C14-SB concentration	1	8816.7	8816.7	57.95	0.002
TiO_2	1	2904.0	2904.0	19.09	0.012
Error	4	608.6	152.1		
Total	8	84642.9			

concentration of 10.50%, bath temperature (7.05%), and inclusion of TiO_2 (3.5%). The same is tabulated in table 6.

3.3 *Modelling*

In this current study, Minitab 19.2020.1 software is used to analyse the linear regression method to formulate predictive mathematical models for predicting the microhardness value of the coatings in response to the input parameter bath temperature, bath pH, addition of surfactant, and TiO_2. The predictive equations deduced from the regression analysis

$$\text{Micro Hardness} = 609 - 7.88\ \text{temperature} + 52.58\ \text{pH} + 4259\ \text{Surfactant} + 88.0\ TiO_2 \quad (2)$$

The developed model adaptivity is verified by the coefficient of determination R^2 values [31]. The R^2 value continuously varies from 0 to 1. The more the R^2 value approaches towards 1, the more a proper fit between independent and dependent variables. For example, assume if $R^2 = 95\%$, then this implies that the predicted observation apprised with 95% variability. In this study, the coefficient of determination is deduced as 98.56%. Furthermore, the residual plot is applied to verify the dominance of the coefficients in the predicted model. If the residual plot lies in a straight line, indicates residual errors from the model are predominantly contributed, and coefficients in the model are significant, the residuals plots traced for ENi-TiO_2 hardness as shown in figure 2. it is ascertained that the residuals disposed near the straight line which affirms that the development coefficient model is significant.

3.4 *Confirmation test*

The confirmation run coating was fabricated with the identified optimal process parameters (i.e., Temperature-80 °C, pH-8, C14SB concentration-0.027 g/L, and Nano TiO_2-

0.75 g/L) to evaluate the repeatability of this study. As a result, the S/N ratio of the optimum level is

$$\overline{Y} = Y_m + \Sigma_i^{\circ} = 1\left(\overline{Y}_1 - Y_m\right) \quad (3)$$

In which $\overline{Y}$ is the overall mean S/N ratio, Y_m is the S/N ratio for deduced optimal parameter combination, and Σ_i° is the quantity of the main parameter.

Table 7 compares the S/N ratio between initial, experimental, and confirmation run results. This result is justifiable and validates the predicted S/N ratios obtained through Taguchi DOE. The confirmation results proved that the enhancement of the S/N ratio was achieved at about 3.7879 dB with an increment of 54.66% in microhardness value through optimal parameters. Additionally, a significant positive correlation was also observed between the microhardness of the optimal coating and the other composite coating synthesised through the Taguchi L9 orthogonal design. The confirmation test confirmed that the orthogonal array and ANOVA results were highly decisive in deducing the better design conditions of Titanium-based Electroless composite coatings to achieve higher hardness in the coatings.

Figure 3 shows the EADX micrograph analysis of four different coated specimens for comparison which containing (a) acidic bath (T-90 °C, pH-4.5), (b) Alkaline bath (T-85 °C, pH-8), (c) T-9 (T-88 °C, pH-8, 0.018 g/L, 0.25 g/L), and (d) T-3 sample (T-80 °C, pH-8, 0.270g/L, 0.75 g/L). Electroless plating was performed more quickly in an alkaline bath than in an acidic bath. Therefore, its deposition rate increases by increasing the pH in each bath condition. It is possible to deduce this from the equation below. As pH increased, Le Chatelier's principle compelled the reactions forward. Apart from nickel deposition and hydrogen evolution, phosphorous was also deposited as a byproduct of nickel deposition.

$$H_2PO_2^- + H \rightarrow H_2O + OH^- + P \quad (4)$$

The elemental composition data obtained through EDAX analysis is shown in table 8. This table fairly reveals several ways; a significant positive correlation between pH and percentage of phosphorous was observed. While comparing the wt% of phosphorous content and its corresponding microhardness valve obtained through the experiment both in the optimal T-3 and T-9 specimens, the phosphorous content of T-3 coating is 9.04 % compared with 10.01 wt% of T-9 coating. It is why the microhardness of the T-3 coating is higher than the T-9 coating. This outcome also exactly supports the evidence from previous observations of Fayyad *et al* [32]. Correlating the higher microhardness value observed on the optimal (T-3) specimen and its corresponding lower Nickel content than the other three compared variants, these results perfectly support the earlier findings of Muraliraja *et al* [23], who experimentally proved that the higher the nickel content reduces the microhardness of the deposits.

Table 7. Confirmation test report

		Optimal condition	
Level	Initial condition A2B2C2D2	Predicted A1B3C1D3	Experimented A1B3C1D3
Weight loss (g)	0.0131	0.0083	0.0085
S/N ratio (dB)	37.6546	41.6184	41.411

3.5 *Effect of C14-SB surfactants on the TiO_2 content*

C14SB Surfactant lowers the surface tension of a liquid, allowing the easier spreading of metals particles, and lowering the interfacial tension between two liquids or a liquid and solid surface. In an electroless nickel bath, the presence of surfactant promotes the coating deposition reaction between the bath solution and the immersed substrate surface [21]. The correlation between the percentage of titanium content in the T-3 and T-9 specimens was interesting. Even though higher TiO_2 nanoparticles (0.75 g/L) were added to the electrolyte for the T-9 specimen, the EDAX micrographs and their elemental compositions interpreted through table 8 reveal the alternate way. Only 0.11 by weight percentage was mapped from the optimal specimen (T-3), and 0.41 by wt% is observed on T-9 samples. In contrast, though the lower concentration of TiO_2 nanoparticles (0.25 g/L) was added to the electrolyte devised for the T-9 specimen, the incorporation of higher titanium content than the T-3 specimen helped us to understand the significance of the surfactant concentration and its CMC value. Furthermore, while decoding the same, a strong association between the chemical composition of ENi-P-TiO_2 deposits and the CMC level of surfactant was corroborated by the similar studies undertaken by Tamilarasan *et al* [33]. He observed from his study and stated that the titanium content in the Ni–P matrix would increase with the increase of surfactant till its CMC value, beyond which the TiO_2 content reduces against any further increase of the surfactant. Thus, the excess surfactant in the bath will envelop the particles and restrict their embedment into the Ni–P matrix. Accordingly, when comparing T-3 and T-9 bath parameters, the CMC value of 0.018 g/L C14SB surfactants was added to the T-9 specimen, and 0.027 g/L was added to the T-3 specimen. Hence, the lower TiO_2 content mapped through EDAX micrographs shown in figure 4 confirms this fact.

Also, the most striking observation is when comparing the microhardness value of the T-3 and T-9 specimens with their elemental compositions. Though the 0.41 wt% of titanium content prevailed in the T-9 deposits, however, its microhardness value is comparatively 27.05% lower than the identified optimal coating (T-3), whose titanium

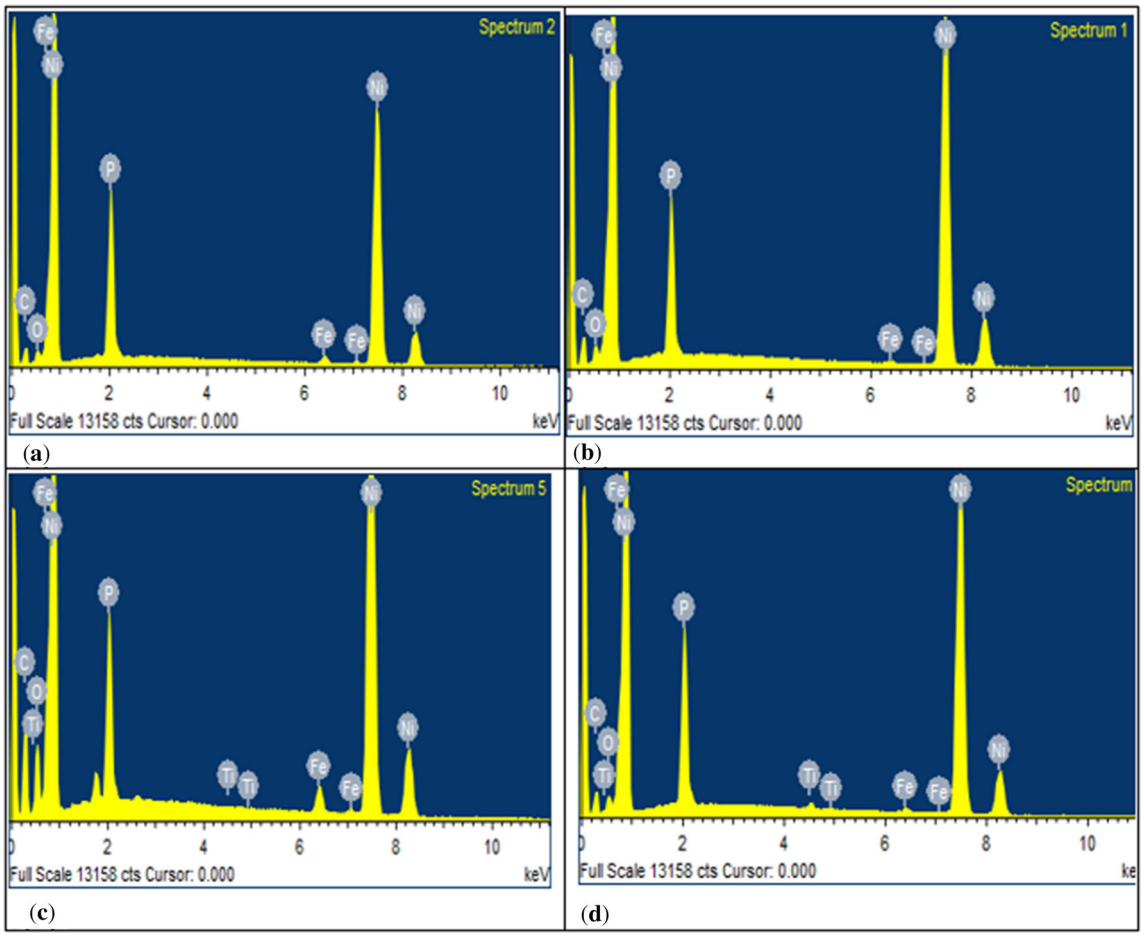

Figure 3. EDAX Micrographs (**a**) ENi-P (acidic), (**b**) ENi-P (alkaline), (**c**) ENi-P-TiO_2 (T-9), (**d**) ENi-P-TiO_2 (T-3).

Table 8. Coatings parameters and elemental composition by weight % (EDAX).

Sl. no.	Coating	Deposition rate (μm/h)	Hardness (HV_{200})	P (wt%)	Ni (wt%)	Ti (wt%)	O (wt%)
1	ENi-P (90°C, pH 4.5 (Acidic))	8.7	310	11.86	71.10	–	1.77
2	ENi-P (85 °C, pH 8 (Alkaline))	22.9	460	8.26	73.61	–	1.96
3	T-3 (80 °C, pH 8, 0.0270 g/L, 0.75g/L) (Optimal coating)	17.7	584	9.04	68.58	0.11	1.87
4	T-9 (88 °C, pH-8, 0.018 g/L, 0.25g/L)	18.6	426	10.01	71.97	0.41	1.80

content is only 0.11 wt% as per the EDAX micrographs shown in figure 3c and d. It is due to Titanium dioxide's inherent mechanical properties, which is comparatively highly (0.41%) embedded in the T-9 than in the T-3 specimen. These results further confirm and support the evidence from the previous observations of Saravanan *et al* [34].

3.6 *Effect of C14-SB surfactants on the deposition rate*

Table 8 and figure 4 interpret the role of surfactant loading and the deposition rate of the ENi-P (acidic), ENi-P (alkaline), and 09 in number Taguchi run ENi-P-TiO_2 deposits. The S-1 and S-2 specimens are fabricated with the

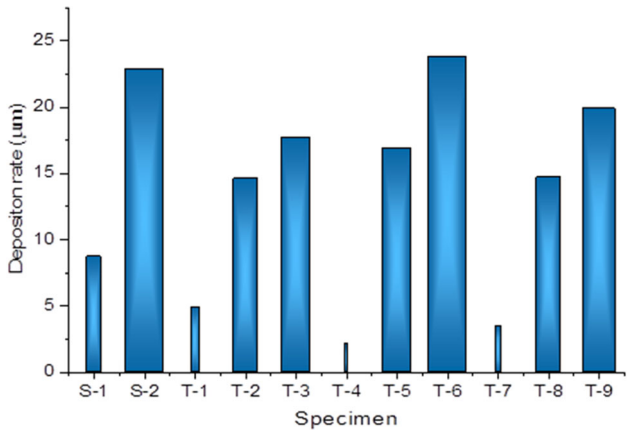

Figure 4. Specimen versus deposition rate.

zwitterionic surfactant at the CMC level, and the remaining specimen is fabricated with 0.5 CMC,1 CMC, and 1.5 CMC loading zwitterionic surfactant for the correlation study. It is indeed evident through the graph that the weight addition of surfactant influences the deposition rate of the coatings in a significant way. The deposition rate decreases with an increase in surfactant loading. The resulting decrease in the deposition rate is attributable to the surfactant molecules being prone to masking the substrate surface, which further restricted the propagation of nickel ions towards the substrate surface, thereby downsizing its deposition rate [33].

Furthermore, beyond the CMC level of the surfactant addition, the electrolyte attains its saturated condition due to the complete isolation of TiO_2 particles by the surfactant molecules, which in turn forms a complete envelope around the particles. The overloading of surfactant further induces a layer over the substrate, resulting in the reduced deposition rate of Nickel and TiO_2 particles. This can be quickly corroborated by the EDAX micrographs (figure 3) and their elemental content tabulated in table 8.

3.7 *Effect of C14-SB surfactants on microhardness of the coatings*

Table 4 also interprets the coating's surfactant addition and corresponding microhardness value. The outcome affirms that the concentration of C14SB surfactant in the electroless bath also plays a pivotal role in determining the microhardness of the ENi-P coatings and further corroborates the findings from Muraliraja *et al* [23]. The earlier reported that the CMC level of C14SB surfactant is 0.018g/L. Further, he proved that incorporating the third element into the ENi-P matrix increases with the addition of the C14-SB surfactant till its CMC level, beyond which the agglomeration observed and hardness reduces due to increasing nickel content in the coating. The same corroborates that the surfactant added in the T-3 sample is 0.0270 g/L which is more than its CMC level of 0.018 g/L. The fact is precisely supported in table 8. When considering the microhardness values of acidic, alkaline, T-3 (optimal), and T-9 specimens, it is evident that significant micro hardness enhancement was achieved on the optimal specimen (T-3), about 196.44% higher than its bare AH36 steel substrate. Furthermore, comparing the microhardness value of acidic and alkaline coatings (coated in the absence of surfactant) with the optimal coating (T-3), a substantial increase of 46.91% and 26.95% were achieved, respectively. Phosphorous content having very low solid solubility in nickel increases excess strain generated in the nickel lattice. This may result in lattice disorder and consequent reduction of hardness. In the present case, the hardness values of the coated surface were found to decrease due to the increase in phosphorus content [35]. Furthermore, Sha *et al* [36] observed that the microhardness of the electroless coated deposits could be decreased as the phosphorous content is progressively increased from 3 to 14% by weight.

3.8 *Influence of bath pH on the surface properties of electroless coatings*

The most important aspect of the data from table 8 and figure 5 is that when observing the bath details of ENi-P (alkaline), T-3(optimal), and T-9 (ENi-P-TiO_2) composite coatings, all these specimens are attained microhardness values above 400 HV_{200} are surprisingly synthesised at pH 8 even though remaining factors are not in common. When the surfactant is added at a CMC value at a higher temperature, the added TiO_2 particles will attract more particles toward the substrate. Also, while interpreting figure 5, Taguchi run specimens T-1, T-4 and T-7 are synthesized with bath pH 4, T-2, T-5, and T-8 specimens fabricated with pH 6, and T-3, T-6, T-9 with pH 8. Interestingly, when comparing the microhardness values of specimens segregated with the pH group-wise (4, 6 and 8), the maximum hardness achieved by specimen T-1 from the pH 4 is 304 HV_{200} which is lower than the minimum microhardness value of 331 HV_{200} from the following pH group range, i.e.,

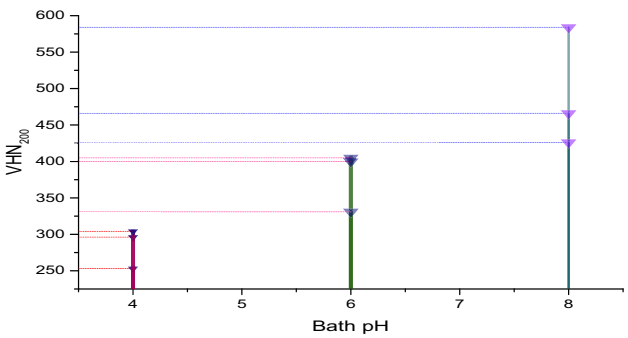

Figure 5. Bath pH versus microhardness.

specimen T-8. Likewise, the maximum microhardness value of 405 HV_{200} gained by specimen T-2 from the pH 6 group is lower than the minimum of 426 HV_{200} gained by specimen T-9 from the pH 8 group. Finally, the optimal combination of this experiment is achieved by the specimen T-3 from the pH 8 group only. Hence, the bath pH played a significant role in achieving the microhardness value in the ENi-P-TiO_2 coatings.

This finding is consistent with the earlier finding of shahil Julka *et al* [28]. Who stated that the elemental composition of the ENi-P composite coating is acutely influenced by changing the bath pH, which plays a determinant role in incorporating the third element in the deposits. The most relevant theory which supports this fact is that the maximum incorporation of particles is achieved when deposition occurs in an Alkaline bath. It is consistent with the earlier findings of Bund *et al* [37].

3.9 *Morphology and X-ray diffraction analysis*

Figure 6 reveals the SEM images of ENi-P (acidic and alkaline) coatings without the second phase and ENi-P-TiO_2 (T-9 and optimal T-3) coatings. The micro-cracks were observed in figure 6a acidic based coatings due to the higher evolution of hydrogen during the deposition process. However, in alkaline deposits of ENi-P in figure 6b, the microcracks are minimal. However, in the case of an Optimal (T-3) coated surface (figure 6d), it is evident that numerous spherical protuberance was observed on the surface with minimal TiO_2 adsorption the surface. Therefore, it can be suggested that the agglomeration of TiO_2 particles occurred due to the addition of Zwitterionic surfactant beyond its CMC level in the electroless bath leading to its minimal deposition. However, in the case of the T-9 specimen, whose fabrication was carried out with the addition of the surfactant at a CMC value of 0.018/L, it led to achieving more second phase presence figure 6c with the non-globulus surface. It is due to the incorporation of TiO_2 into the Ni-P matrix disturbs the heterogeneity of the deposits and further propagates numeral boundaries between the nickel and phosphorous in the coatings, thereby resulting in a lower microhardness value.

Figure 7 compares the XRD plots of substrate material (AH36), T-9 specimen, and ENi-P-TiO_2 optimal(T-3) coated surface (as-deposited). The diffraction profiles available Fe_7C and Fe_3C phases are from the AH36 steel. Likewise, the ferrous profiles observed on the composite coatings are from the AH36 steel underneath the coating.

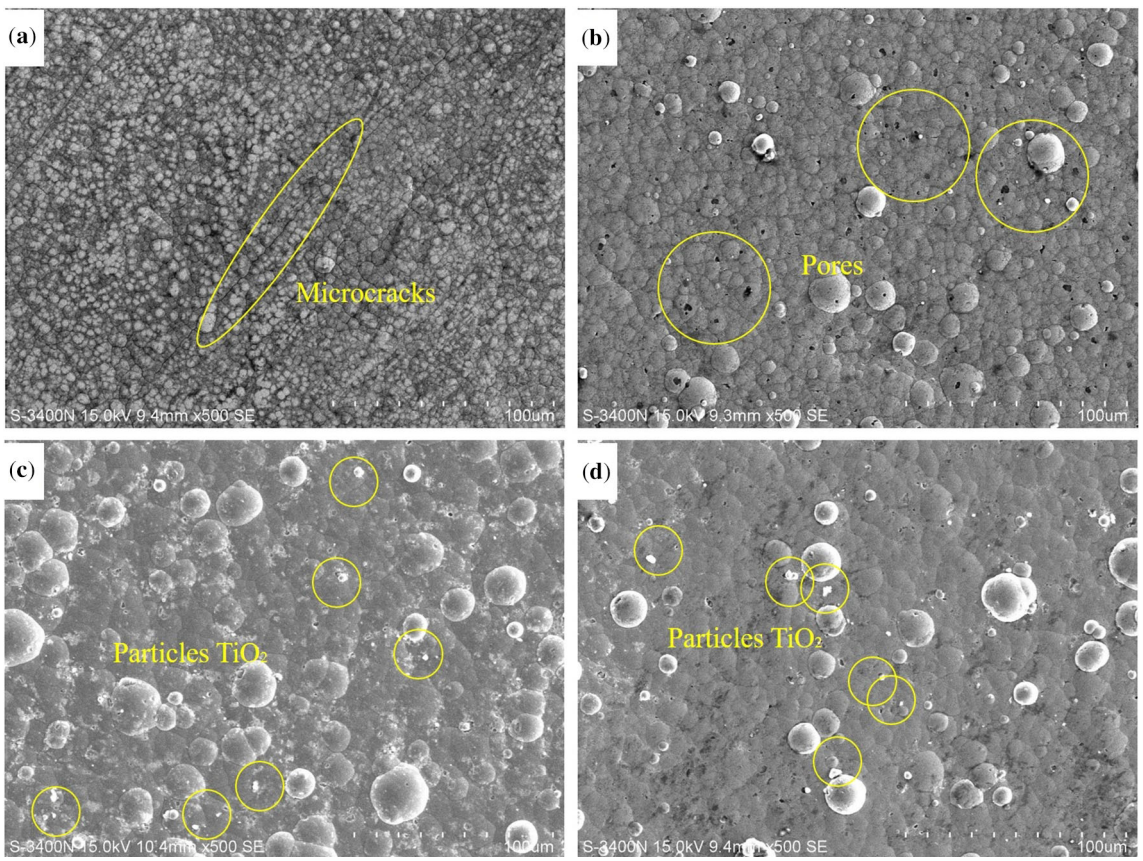

Figure 6. SEM images (**a**) ENi-P (Acidic); (**b**) ENi-P(Alkaline); (**c**) ENi-P-TiO_2 (T-9); (**d**) ENi-P-TiO_2 (T-3).

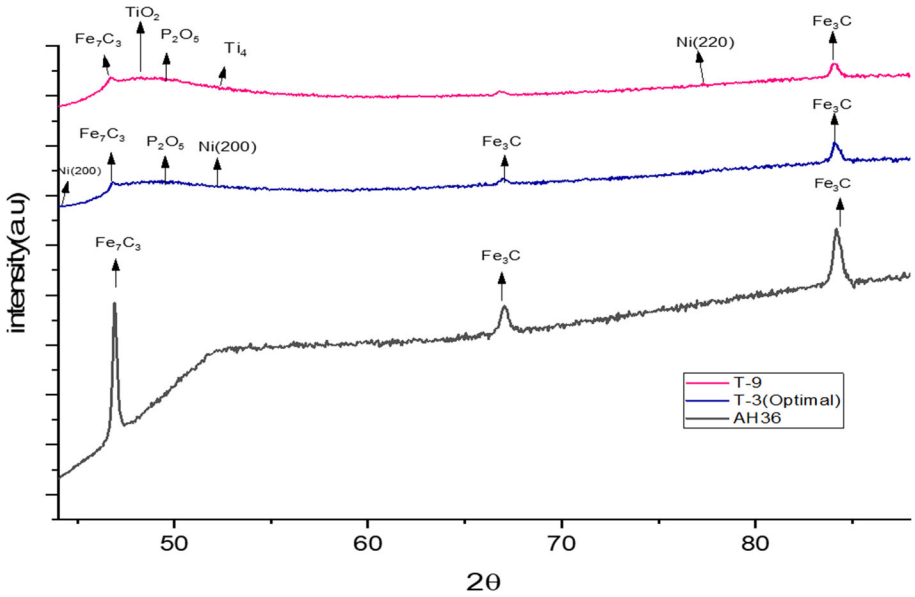

Figure 7. XRD Plots of base material and ENi-P-TiO_2 coatings.

The XRD profile of both the ENi-P-TiO_2 reveals amorphous formation and Nickel, Phosphorous, and Titanium phases on the coated surface. However, the diffraction from Nickel {111} is not visible due to being excessively overlapped by the presence of an amorphous profile in the coated layer. These results align with the earlier findings of Sha et al [36] and are consistent with the existing literature. However, Nickel {200} and {220} are visible in both the coated surface. Alternately, the reflections of TiO_2 and Ti_4 are visible in the T-9 XRD profile; such reflection is not visible in the T-3 optimal coating profiles. Notwithstanding with EDAX micrograph, which affirms the presence of TiO_2 in the T-3 deposits, the diffraction peaks of second phase titanium not detected from the surface are conceivably due to its minimal incorporation in the coating. Furthermore, the EDAX elemental composition results in table 8 affirm the same. Most obviously, the intensity of the Fe_3C phase in the composite coatings is minimal compared with the XRD profile of AH36 steel due to the coating thickness over the base metal (AH36), and total absorption of penetrated X-ray is not feasible due to its minimal thickness. Furthermore, while comparing the T-3 and T-9 profiles, the intensity of the Fe3C phase in the T-3 coatings is higher than the T-9 coatings due to its lower thickness than the latter [36].

4. Conclusions

The titanium-based ENi-P composite deposition with the varying bath temperature, bath pH, Zwitterionic surfactant, and nano-TiO_2 are fabricated on AH36 based on Taguchi L9 design. The present study was designed to identify the determinant factor and their optimal parameter combination for achieving high microhardness in the deposition. The outcome of this study is as follows:

(1) The finding from this study provides insights for adopting environmentally friendly Electroless coating on Naval grade steel AH36 steel. Accordingly, acidic and alkaline ENi-P coatings and L9 titanium-based ENi-P composite coatings were fabricated and compared with the AH36 substrate material to evaluate surface properties enhancement through microhardness and morphological investigations.

(2) ANOVA analysis revealed that bath pH contributed substantially at about (78.95%) to enhancing microhardness in the deposited ENi-P-TiO_2 surfaces.

(3) In this investigation, the relation between the microhardness of the coatings and their corresponding bath pH is observed. Accordingly, all nine specimens are divided into three groups with respect to their bath pH (4, 6, and 8), and when analysed, the microhardness value of all three specimens from pH group 6 is higher than the variants of pH group 4; consequently, the microhardness values of all three variants of pH 8 is higher than the remaining two group specimens. Furthermore, the optimal coating to achieve maximum microhardness is identified from pH 8 only.

(4) The confirmation run experimentation results from the optimal combination (A1B3C3D3) show that enhancement of the S/N ratio was achieved at about 3.7879 dB, and a rise of 54.66% of microhardness was achieved when compared with the initial condition. Furthermore, a significant positive correlation was observed between phosphorous content and the microhardness of the coatings.

(5) The evidence from the XRD diffractogram has significant implications for understanding how the CMC value of added Zwitterionic surfactants in the electroless bath affects the inclusion of titanium particles in the Ni–P matrix.
(6) Furthermore, the current study is the first kind of investigation of deposition of novel ENi-P-TiO_2 electroless coating on marine grade AH36 steel, and it further lays the groundwork for future research on fabricating this novel coatings technique for marine applications.

Acknowledgements

One of the authors, R Anthoni Sagaya Selvan, would like to thank Prof. V. Balasubramanian, Director of Centre for Materials Joining and Research (CEMAJOR), Head of the Department of Manufacturing Engineering, Faculty of Engineering & Technology, Annamalai University, to extend lab facilities to conduct this study during ongoing pandemic situations. Furthermore, without the exceptional support of Comdt (JG) AK Pandey, Commanding Officer, ICGS Ameya, Indian Coast Guard, it would not have been possible to complete this study successfully.

References

[1] Ribeiro A C N, Henein H, Ivey D G and Brandi S D 2016 Evaluation of AH36 microalloyed steel welded joint by submerged arc welding process with one and two wires. *Mater. Res.* 19(1): 143–152
[2] Igi S, Inohara Y and Hirai T 2005 High performance steel plates for shipbuilding—Life cycle cost reduction technology of JFE Steel. *JFE Tech. Rep.* 5(5): 16–23
[3] Nogueira I, Dias A M, Gras R and Progri R 2002 An experimental study to corelate water jet impingement erosion resistance and properties of metallic materials and coatings. *Wear* 253(5–6): 650–661
[4] Ivce R, Grubiša M and Mišković D 2019 Protection coatings for the underwater part of ship's hull. *J. Marit. Transp. Sci.* 55(1): 59–70
[5] Brenner A and Riddel G E 1953 United States Patent Office, Nickel Plating by Chemical Reduction. 8–9
[6] Weil R and Parker K 2000 Chapter 4 The properties of electroless Nickel. *Plating*. 111–137
[7] Zhang P, Li S X and Zhang Z F 2011 General relationship between strength and hardness. *Mater. Sci. Eng. A* 529(1): 62–73
[8] Li Y P, Zhu X F, Zhang G P, Tan J, Wang W and Wu B 2010 Investigation of deformation instability of Au/Cu multilayers by indentation. *Philos. Mag.* 90(22): 3049–3067
[9] Gadhari P and Sahoo P 2016 Electroless nickel-phosphorus composite coatings: A review. *Int. J. Manuf. Mater. Mech. Eng.* 6(1): 14–50
[10] Sudagar J, Lian J and Sha W 2013 Electroless nickel, alloy, composite and nano coatings—A critical review. *J. Alloys Compd.* 571: 183–204
[11] Balaraju J N, Sankara Narayanan T S N and Seshadri S K 2003 Electroless Ni–P composite coatings. *J. Appl. Electrochem.* 33(9): 807–816
[12] Dong D, Chen X H, Xiao W T, Yang G B and Zhang P Y 2009 Preparation and properties of electroless Ni–P–SiO_2 composite coatings. *Appl. Surf. Sci.* 255(15): 7051–7055
[13] Alirezaei S, Monirvaghefi S M, Salehi M and Saatchi A 2004 Effect of alumina content on surface morphology and hardness of Ni–P–$Al_2O_3(\alpha)$ electroless composite coatings. *Surf. Coat. Technol.* 184(2–3): 170–175
[14] Araghi A and Paydar M H 2010 Electroless deposition of Ni–P–B_4C composite coating on AZ91D magnesium alloy and investigation on its wear and corrosion resistance. *Mater. Des.* 31(6): 3095–3099
[15] Novakovic J, Vassiliou P, Samara K and Argyropoulos T 2006 Electroless NiP–TiO_2 composite coatings: Their production and properties. *Surf. Coat. Technol.* 201(3–4): 895–901
[16] Allahkaram S R, Salmi S and Tohidlou E 2012 An investigation on effects of TiO_2nano-particles incorporated in electroless nip coatings' properties. *Int. J. Mod. Phys. Conf. Ser.* 5: 833–840
[17] Hamid Z A, El Badry S A and Aal A 2007 Electroless deposition and characterization of Ni–P–WC composite alloys. *Surf. Coat. Technol.* 201(12): 5948–5953
[18] Chen W, Gao W and He Y 2010 A novel electroless plating of Ni–P–TiO_2 nano-composite coatings. *Surf. Coat.ings Technol.* 204(15): 2493–2498
[19] Tamilarasan T R, Sathish Kumar R, Rajendran R and Rajagopal G 2015 Optimization of electroless Ni–P–nano-TiO_2 coating parameters using Taguchi method for corrosion performance. *Appl. Mech. Mater.* 813–814: 95–100
[20] Shozib I A, Ahmad A, Rahaman M S A, Abdul-Rani A M, Alam M A, Beheshti M and Rahman I T 2021 Modelling and optimization of microhardness of electroless Ni–P–TiO_2 composite coating based on machine learning approaches and RSM. *J. Mater. Res. Technol.* 12: 1010–1025
[21] Sahoo P and Das S K 2011 Tribology of electroless nickel coatings—A review. *Mater. Des.* 32(4): 1760–1775.
[22] Elansezhian R, Ramamoorthy B and Kesavan Nair P 2008 Effect of surfactants on the mechanical properties of electroless (Ni–P) coating. *Surf. Coat. Technol.* 203(5–7): 709–712
[23] Muraliraja R, Elansezhian R, Sudagar J and Raviprakash A V 2016 Influence of a zwitterionic surfactant on the surface properties of electroless Ni–P coating on mild steel. *J. Surfactants Deterg.* 19(5): 1081–1088
[24] Bückle H 1959 Progress in micro-indentation hardness testing. *Metall. Rev.* 4(1): 49–100
[25] Sahoo P 2009 Wear behaviour of electroless Ni–P coatings and optimization of process parameters using Taguchi method. *Mater. Des.* 30(4): 1341–1349
[26] Dean E B and Unal R 1991 Taguchi Approach to Design Optimization for Quality and Cost: An Overview. *Annu. Conf. Int. Soc. Parametr. Anal.* 1–10
[27] Sarkar S, Baranwal R K, Banerjee S, Prakash A, Mandal R and Majumdar G 2018 Parametric optimization of process parameters on the response of microhardness of electroless

Ni–P coating. *J. Mol. Eng. Mater.* 6(1–2): 1850003

[28] Julka S, Ansari M I and Thakur D G 2016 Effect of pH on mechanical, physical and tribological properties of electroless Ni–P–Al_2O_3 composite deposits for marine applications. *J. Mar. Sci. Appl.* 15(4): 484–492

[29] Seeman M, Kanagarajan D, Sivaraj P, Seetharaman R and Devaraju A 2019 Optimization through NSGA-II during machining of A356Al/20%SiCp metal matrix composites using PCD Tool. *IOP Conf. Ser. Mater. Sci. Eng.* 574: 012008

[30] Seeman M, Ganesan G, Karthikeyan R and Velayudham A 2010 Study on tool wear and surface roughness in machining of particulate aluminum metal matrix composite-response surface methodology approach. *Int. J. Adv. Manuf. Technol.* 48: 613–624

[31] Seeman M, Sivaraj P, Seetharaman R and Ashok Kumar I 2020 Analysis and optimization of machining parameter during turning of A356/10%SiCp MMC using response surface methodology approach. *IOP Conf. Ser. Mater. Sci. Eng.* 961: 012014

[32] Fayyad E M, Abdullah A M, Hassan M K, Mohamed A M, Jarjoura G and Farhat Z 2018 Recent advances in electroless-plated Ni–P and its composites for erosion and corrosion applications: A review. *Emerg. Mater.* 1(1–2): 3–24

[33] Tamilarasan T R, Rajendran R, Rajagopal G and Sudagar J 2015 Effect of surfactants on the coating properties and corrosion behaviour of Ni–P–nano-TiO_2 coatings. *Surf. Coat. Technol.* 276: 320–326

[34] Saravanan I, Elayaperumal A, Devaraju A, Karthikeyan M and Raji A 2020 Wear behaviour of electroless Ni–P and Ni–P–TiO_2 composite coatings on En8 steel. *Mater. Today Proc.* 22(3): 1135–1139

[35] Shibli S M A and Dilimon V S 2007 Effect of phosphorous content and TiO_2-reinforcement on Ni–P electroless plates for hydrogen evolution reaction. *Int. J. Hydrog. Energy.* 32(12): 1694–1700

[36] Sha W, Wu X and Keong K G 2011 Electroless copper and nickel-phosphorus plating: Processing, characterisation and modelling. Woodhead Publishing Limited, Cambridge

[37] Bund A and Thiemig D 2007 Influence of bath composition and pH on the electrocodeposition of alumina nanoparticles and copper. *J. Appl. Electrochem.* 37(3): 345–351